

Mathematical Modelling of a Rotating Deformable Space Vehicle Lase Attitude Motions

Saraka Jean Modeste Kouassi^a, Moussa Sylla^{b*}

^a*UFR Mathématiques et Informatique Université Félix Houphouët-Boigny Laboratoire de Mécanique*

^b*UFR Mathématiques et Informatique Université Félix Houphouët-Boigny Laboratoire de Mécanique, Abidjan, 22 BP 582, Côte d'Ivoire*

^a*Email: ksarakajm@yahoo.fr*

^b*Email: ba_mouss@yahoo.fr*

Abstract

A rotating elastic space vehicle composed of a central rigid body connected to two solar arrays, subjected to external torques, is studied using the spectral expansion continuum method of Rayleigh-Ritz. The lase attitudes motion of the rotating space vehicle can be described by a linear combination of the global modes different from the usual ordinary modes. By application of the spectral expansion continuum approach of Rayleigh-Ritz, the impedance function of the space vehicle in terms of the global modes of the whole system is derived. The numerical simulation of these global modes of great interest in this study, are performed by means of this impedance function relating the external torques to the rotating space vehicle lase attitudes.

Keywords: vibration; global mode; spectral expansion; impedance function.

1. Introduction

Several papers using the spectral decomposition continuum approach of Rayleigh-Ritz [1-12] are interested by the attitudes motions of elastic multibody system in dynamics. Many authors use different mathematical models to perform the modal analysis of the mechanical system attitudes motion. These attitudes motions are supposed to be coupled and expanded generally with the choice of the non-rotating base cantilever modes [2, 3, 5, 7, 8, 9, 11, 12] or the rotating base cantilever modes [1, 4, 6, 7, 10]. The modes used by the authors to describe the distributed flexibility of the mechanical system, leads to the spectral expansion of the reduced impedance matrix of the multibody system deriving from this analysis. The external torques exerted on the multibody system are related to its coupled attitudes by means of this matrix.

* Corresponding author.

The present investigation uses the spectral decomposition continuum approach of Rayleigh-Ritz. One describes the dynamics of a simplified elastic space vehicle composed of a central rigid body connected to two flexible solar arrays. The particularity in this work, is the decoupling between the attitudes motions of the spacecraft, which phenomena can be observed physically due to the effect of attitudes control. In this case, the interest is put on the lace attitude motions interacting with the flexible parts global modes [12]. From the spectral decomposition theory performed, one gets the impedance function of the whole system. Hence, by means of numerical algorithm using this impedance function, the global modes frequencies and the natural vibrations frequencies of the whole space vehicle are computed. In the modal analysis, one supposes that the elastic space vehicle undergoes small lace attitudes motions and elastic vibrations motions interacting with its rotating orbital motion, around an equilibrium corresponding to some gravity-gradient stabilized position where the flexible appendages are undeformed [7, 13].

2. Dynamical equations of the space vehicle

2.1. Formulation and parameterization of the space vehicle motion

The mechanical system (\mathfrak{B}) studied is composed of a central rigid body (\mathfrak{B}_0) linked symmetrically to two solar arrays (\mathfrak{B}_1) and (\mathfrak{B}_2) by means of two rigid pieces (γ_1) and (γ_2) in two points O_1 and O_2 respectively. Each array (\mathfrak{B}_i) ($i = 1$ or 2) is composed of a supporting piece (SP_i), a membrane (BL_i) and a tip piece (TP_i). The solar arrays have the same physical characteristics. One notes $\mathfrak{R}(t) = (O_0; \vec{X}_0, \vec{Y}_0, \vec{Z}_0)$ the central reference frame which is rigidly joined to (\mathfrak{B}_0) of mass center O_0 . $\mathfrak{R}_G = (G; \vec{a}, \vec{b}, \vec{c})$ is the orthonormal orbiting reference of origin G which is the mass center of the whole system deformed. The solar arrays are modelled by rectangular membranes of constant surface density σ . The width and length of each solar array in its underformed position are denoted by e and l respectively. The plane $(O_0; \vec{X}_0, \vec{Z}_0)$ designates the whole system symmetric plane in its underformed position (see figure 1). The inertial frame reference is denoted by $\mathfrak{R}_T = (T; \vec{X}, \vec{Y}, \vec{Z})$. Relative to \mathfrak{R}_T , the frame \mathfrak{R}_G is spinning around the axis $(T; \vec{Z})$ with a constant angular speed n_0 . During its orbital motion, the frame \mathfrak{R}_G drives the whole space vehicle (\mathfrak{B}) which mass center G is supposed to describe a circular orbit of center T in the plane $(T; \vec{X}, \vec{Y})$ (see figure 2). The equilibrium position of the space vehicle (\mathfrak{B}) with respect to the orbital reference frame is perturbed by its small lace attitude motions of angle $\theta(t)$ interacting with the solar arrays elastic deformations, represented by the vector \vec{d}_i (see figure 4):

$$\vec{d}_i(M, t) = (u_i(s, t), 0, 0)^T; \quad s \in [0; l]; \text{ on } (SP_i); \quad \vec{d}_i(M, t) = (\alpha_i(x, s, t), 0, 0)^T \quad (x, s) \in R; \text{ on } (BL_i).$$

On (TP_i) the displacements field \vec{d}_i are obtained by the boundary condition applied on (BL_i) and (SP_i) . The vector \vec{d}_i is measured in the frame components $\mathfrak{R}(t)$. R is the integration domain representing the rectangular membrane (BL_i) defined as follows:

$$R = \left\{ (x, s) / \frac{-e}{2} \leq x \leq \frac{+e}{2}, 0 \leq s \leq l \right\}.$$

For the remainder, for any function F depending on the spatial variable s and the time t , one notes:

$$\dot{F} = \frac{\partial F}{\partial t}, \ddot{F} = \frac{\partial^2 F}{\partial t^2}, F' = \frac{\partial F}{\partial s}, F'' = \frac{\partial^2 F}{\partial s^2}.$$

2.2. Equations of the space vehicle motion

By the use of the variational principle of Hamilton, one gets the equation of the global motion and the local equations of the flexible appendages motion (see appendix 2):

- Equation of the global motion

$$C\ddot{\theta} + 3n_0^2(B - A)\theta + \dot{N}_u^* + n_0\dot{N}_\alpha^* + 3n_0^2N_u^* = Y.$$

(1)

Where A, B and C are moments of inertia of the space vehicle and Y is the external forces applied to the space vehicle:

$$\begin{cases} N_\alpha^* = 2 \sum_{i=1}^2 \left[\int_0^l \sigma x \alpha_i(x, s, t) ds \right] \\ N_u^* = \sum_{i=1}^2 (-1)^i \left[\int_0^l \rho(b + s) u_i(s, t) ds + \sigma \iint_R (b + s) \alpha_i(x, s, t) dx ds + \tilde{m}(b + l) u_i(l, t) \right] \end{cases}$$

(2)

- Local motions equations of each solar array ($B_i, i = 1, 2$)

$$\rho[\ddot{u}_i + (-1)^i(b + s)(\ddot{\theta} + 3n_0^2\theta)] + [\tilde{P}(s)u_i']' + Elu_i^{(4)} = 0 \text{ into } (SP_i),$$

(3)

$$\sigma[\ddot{\alpha}_i - 2n_0x\dot{\theta} + (-1)^i(b + s)(\ddot{\theta} + 3n_0^2\theta)] - \{[\tilde{G} + \tilde{T}(s)]\alpha_i'\}' = 0 \text{ into } (BL_i),$$

(4)

$$\tilde{m}[\ddot{u}_i(l, t) + (-1)^i(b + l)(\ddot{\theta} + 3n_0^2\theta)] - Elu_i^{(3)}(l, t) - Pu_i'(l, t) + [\tilde{G}e + P + 3n_0^2\tilde{m}(b + l)]\alpha_i'(l, t) = 0 \text{ on}$$

(TP_i).

(5)

Here:

$\tilde{P}(s)$ is the dynamic stiffness exerted at any material point $M(s)$ of (SP_i):

$$\tilde{P}(s) = P - 3\rho \frac{n_0^2}{2} [(b + l)^2 - (b + s)^2].$$

(6)

P is the constant compression applied to the supporting piece (SP_i).

$\tilde{T}(s)$ is the dynamic stiffness exerted to any material point M of (BL_i) :

$$\tilde{T}(s) = \frac{P}{e} + 3 \frac{n_0^2}{2} \left[\sigma(b+l)^2 - \sigma(b+s)^2 + 2 \frac{\tilde{m}}{e} (b+l) \right]. \quad (7)$$

$$\tilde{G} = \frac{Eh}{4(1+\nu)}.$$

E is the Young modulus, ν is the Poisson ratio of the membranes, h is the thickness of the blanket (BL_i) .

- Boundary conditions of the problem

The geometrical conditions on the boundary between the rigid interface (γ_i) and the solar array (B_i) , relative to the displacement fields $u_i(s, t)$ and $\alpha_i(x, s, t)$ of (SP_i) and (BL_i) respectively, are defined by:

$$\begin{cases} u_i(0, t) = 0 \\ \alpha_i(x, 0, t) = 0. \\ u_i'(0, t) = 0 \end{cases} \quad (8)$$

The continuity of the displacement fields on the boundary between (BL_i) and (SP_i) , is expressed by:

$$\alpha_i(x, l, t) = u_i(l, t). \quad (9)$$

Consequently, one has:

$$\frac{\partial \alpha_i(x, l, t)}{\partial x} = \frac{\partial u_i(l, t)}{\partial x} = 0.$$

From (9), one considers an admissible function α_i independent of the variable x , of the form:

$$\alpha_i = \alpha_i(s, t).$$

The natural condition in absence of external torques exerted on (SP_i) tip, is determined by:

$$u_i''(l, t) = 0. \quad (10)$$

3. Resolution of the global modes equations

3.1. Analytical forms of the shape functions

The global modes are the solutions obtained by setting the following conditions in the equations (1), (3), (4) and (5):

$$Y = 0, n_0 = 0.$$

(11)

In this case, the space vehicle attitudes motion are decoupled. Here, one recalls that the interest is put on the lace attitude motion of the space vehicle interacting with the solar arrays bending in plane. The global modes solutions proposed are of the forms:

$$\begin{cases} \theta(t) = \theta_n \cos(\varphi_n t) \\ u_i(s, t) = U_{ni}(s) \cos(\varphi_n t) \\ \alpha_i(s, t) = \alpha_{ni}(s) \cos(\varphi_n t) \end{cases} .$$

(12)

with:

$$\begin{cases} U_{ni}(s) = (-1)^i \theta_n U_n^*(s) \\ \alpha_{ni}(s) = (-1)^i \theta_n \alpha_n^*(s) \end{cases} ; \quad n = 1, \dots, \infty.$$

(13)

One gets, from the resolution of the equations (3) and (4), the following solutions:

$$\begin{cases} U_n^*(s) = a_n \cosh(\psi_n s) + b_n \sinh(\psi_n s) + (b - a_n) \cos(\phi_n s) \\ \quad + \frac{1 - b_n \psi_n}{\phi_n} \sin(\phi_n s) - b - s \\ \alpha_n^*(s) = c_n \sin(\xi_n s) + b \cos(\xi_n s) - b - s \end{cases} ,$$

where:

$$\psi_n = \sqrt{-\frac{P}{2EI} + \sqrt{\left(\frac{P}{2EI}\right)^2 + \frac{\rho\tau_n^2}{EI}}}; \quad \phi_n = \sqrt{\frac{P}{2EI} + \sqrt{\left(\frac{P}{2EI}\right)^2 + \frac{\rho\tau_n^2}{EI}}};$$

and

$$\xi_n = \varphi_n \sqrt{\frac{\sigma e}{(e\tilde{G} + P)}}.$$

φ_n is the global eigenfrequency associated with the global eigenmodes θ_n , $U_{ni}(s)$ and $\alpha_{ni}(s)$.

3.2. Equation of the eigenfrequencies

The solutions of formula (12) are introduced into the equations of the global motion (1), and taking into account the conditions (11), one obtains from laborious calculations the following equation of the eigenfrequencies:

$$\int_0^l \rho(b+s)U_n^*(s)ds + \sigma e \int_0^l (b+s)\alpha_n^*(s)ds + \tilde{m}(b+l)U_n^*(l) = -\frac{C}{2} \tag{14}$$

The global eigenfrequencies φ_n corresponding to bending in plane, are computed by means of the equation (14).

3.3. Calculation of the lace attitude θ_n

One considers a set of global eigenmodes denoted by (U_{ni}, U_{pi}) , and $(\alpha_{ni}, \alpha_{pi})$, satisfying the following normalized orthogonality property (see appendix 3):

$$\theta_n \theta_p \left[2 \left(\rho \int_0^l U_n^*(s)U_p^*(s)ds + \sigma e \int_0^l \alpha_n^*(s)\alpha_p^*(s)ds + \tilde{m}U_n^*(l)U_p^*(l) \right) - C \right] = \delta_{np} \tag{15}$$

$$\delta_{np} = \begin{cases} 1 & \text{if } n = p \\ 0 & \text{if } n \neq p \end{cases}; n = 1, \dots, \infty; p = 1, \dots, \infty,$$

δ_{np} designates Kronecker symbol.

Using the formula (15), one gets the following expression of the lace attitude θ_n :

$$\theta_n = \left[2 \left(\rho \int_0^l U_n^{*2}(s)ds + \sigma e \int_0^l \alpha_n^{*2}(s)ds + \tilde{m}U_n^{*2}(l) \right) - C \right]^{-\frac{1}{2}} \tag{16}$$

4. General motion of the space vehicle in term of the global modes superposition

The general motion of the space vehicle is governed by the global equation (1) and the local equation (3) and (4) under the following conditions:

$$Y \neq 0 ; n_0 \neq 0 ; \theta(t) \neq 0 ; \alpha_i(s, t) \neq 0 ; u_i(s, t) \neq 0.$$

According to the Rayleigh-Ritz superposition method [1-12], the deformations of the flexible bodies and the lace attitudes of the space vehicle, solutions of these equations are represented by a linear combination of the global eigenmodes known associated with functions called generalized coordinates. It follows:

$$\begin{cases} u_i(s, t) = \sum_{n=1}^{\infty} (-1)^i \theta_n U_n^*(s) g_n(t) \\ \alpha_i(s, t) = \sum_{n=1}^{\infty} (-1)^i \theta_n \alpha_n^*(s) g_n(t) , \\ \theta(t) = \lambda(t) + \sum_{n=1}^{\infty} \theta_n g_n(t) \end{cases} \tag{17}$$

$g_n(t)$ is the generalized coordinates to be determined by the modal analysis. Here, $\lambda(t)$ represents the rigid

response of the whole spacecraft if it were rigid.

4.1. Determination of generalized coordinates

Injecting the expansions (17) of the elastic deformations and the lace attitudes into the local equations (3), (4) and (5) and taking into account the boundary conditions (8), (9) and (10) the normalized orthogonality property (15) and the natural frequencies equation (14), one gets the following differential equation of the generalized coordinates:

$$\ddot{g}_k(t) + \varphi_k^2 g_k(t) + 3n_0^2 \sum_{n=1}^{\infty} m_{nk} g_n(t) = C \theta_k [\ddot{\lambda}(t) + 3n_0^2 \lambda(t)], k = 1, 2, \dots \tag{18}$$

here:

$$m_{nk} = \theta_n \theta_k \left[\int_0^l e^{\tilde{T}_1^*(s)} \alpha_n^{*'}(s) \alpha_k^{*'}(s) ds + \int_0^l \tilde{P}_1^*(s) U_n^{*'}(s) U_k^{*'}(s) ds - C \right], \tag{19}$$

with

$$\tilde{T}_1^*(s) = \sigma(b+l)^2 - \sigma(b+s)^2 + 2 \frac{\tilde{m}}{e} (b+l); \quad \tilde{P}_1^*(s) = \rho[(b+l)^2 - (b+s)^2].$$

One supposes that the generalized coordinates and the rigid response are harmonic of the form:

$$g_n(t) = \hat{g}_n e^{j\Omega t}, \quad \lambda(t) = \hat{\lambda} e^{j\Omega t}, \tag{20}$$

here: Ω is a real parameter to be determined and $j^2 = -1$.

One defines the following column vectors:

$$\underline{\hat{G}}_N^T = (\hat{g}_1, \dots, \hat{g}_N), \quad \underline{\theta}_{-N}^T = (\theta_1, \dots, \theta_N),$$

and the following matrix:

$$\underline{\underline{M}}_N = \begin{pmatrix} \varphi_1^2 + 3n_0^2 m_{11} & 3n_0^2 m_{12} & \dots & 3n_0^2 m_{1k} & \dots & 3n_0^2 m_{1N} \\ 3n_0^2 m_{21} & \varphi_2^2 + 3n_0^2 m_{22} & \dots & 3n_0^2 m_{2k} & \dots & 3n_0^2 m_{2N} \\ \vdots & \vdots & \ddots & \vdots & \ddots & \vdots \\ 3n_0^2 m_{k1} & \dots & \dots & \varphi_k^2 + 3n_0^2 m_{kk} & \dots & 3n_0^2 m_{kN} \\ \vdots & \vdots & \vdots & \vdots & \ddots & \vdots \\ 3n_0^2 m_{N1} & \dots & \dots & 3n_0^2 m_{Nk} & \dots & \varphi_N^2 + 3n_0^2 m_{NN} \end{pmatrix},$$

$$\left(\underline{\underline{M}}_N \right)_{nk} = \varphi_n^2 \delta_{nk} + 3n_0^2 m_{nk}.$$

Equations (18) are written in the following matrix forms:

$$\left[\underline{\underline{M}}_N - \Omega^2 \underline{\underline{I}}_N \right] \underline{\underline{G}}_N = C(3n_0^2 - \Omega^2) \theta_{-N} \hat{\lambda}. \quad (21)$$

$\underline{\underline{I}}_N$ is the unit matrix $N \times N$.

The symmetrical matrix $\underline{\underline{M}}_N$ with respective eigenvalues denoted h_k ($k = 1, \dots, N$) can be diagonalized as:

$$\underline{\underline{M}}_N = \underline{\underline{B}}_N \underline{\underline{H}} \underline{\underline{B}}_N^T, \quad (22)$$

here:

$$\left(\underline{\underline{B}}_N \right)_{nk} = b_{nk},$$

$$\underline{\underline{H}} = \begin{pmatrix} h_1 & \dots & 0 \\ \vdots & \ddots & \vdots \\ 0 & \dots & h_N \end{pmatrix}.$$

The matrix $\underline{\underline{B}}_N$ is orthogonal matrix.

Substituting the factorizations (22) into the equation (21) and assuming that:

$$h_k \neq \Omega^2.$$

One gets finally the generalized coordinates:

$$\hat{g}_n = \hat{g}_n^* \hat{\lambda}, \quad (23)$$

here

$$\hat{g}_n^* = C(3n_0^2 - \Omega^2) \sum_{k=1}^N \left[\frac{b_{nk}}{h_k - \Omega^2} \sum_{v=1}^N b_{kv} \theta_v \right], \quad n = 1, 2, \dots$$

4.2. Determination of the impedance function of the system

By using the expressions (2), the solutions (17), the equations of eigenfrequencies (14), and the Fourier transformation, the equations (1) of the global motion becomes:

$$\{3n_0^2[B - A + (B - A - C) \sum_{n=1}^N \theta_n \hat{g}_n^*] - \Omega^2 C\} \hat{\lambda} = \hat{Y}. \quad (24)$$

One defines the following terms:

$$Z^0(\Omega) = 3n_0^2(B - A) - \Omega^2 C, \quad Z^n(\Omega) = 3n_0^2(B - A - C) \theta_n \hat{g}_n^*, \quad (25)$$

$$Z(\Omega) = Z^0(\Omega) + \sum_{n=1}^N Z^n(\Omega). \quad (26)$$

One can rewrite the equation (24) in the form:

$$Z(\Omega) \hat{\lambda} = \hat{Y}. \quad (27)$$

Here: $Z(\Omega)$ is the impedance function connecting the external forces \hat{Y} and the response $\hat{\lambda}$ of the space vehicle.

Formula (26) is the spectral expansion of the impedance function $Z(\Omega)$.

4.3. Equation of global frequencies

In the absence of external forces, the global motion of the space vehicle is governed by the following equation:

$$Z(\Omega) \hat{\lambda} = 0. \quad (28)$$

One assumes non trivial solution $\hat{\lambda}$ of equation (28). Hence the function $Z(\Omega)$ must necessarily verifies:

$$Z(\Omega) = 0. \quad (29)$$

Equation (29) is the equation of the global eigenfrequencies Ω when the space vehicle undergoes natural free attitude motion interacting with elastic deformations.

4.4. Convergence of the global modes gain

One defines the global modes gain as the following series:

$$\sum_{n=1}^{\infty} \theta_n^2.$$

The modal analysis of the space vehicle equations motion performed using the superposition method of

Rayleigh-Ritz, establishes the convergence of the global modes gain above (see appendix 4):

$$\sum_{n=1}^{\infty} \theta_n^2 = \frac{2\mathcal{L}}{c(c-2\mathcal{L})},$$

(30)

here:

$$\mathcal{L} = \tilde{m}(b+l)^2 + (\sigma e + \rho) \left(b^2 l + bl^2 + \frac{l^3}{3} \right).$$

This convergence property gives an approximation of the modal gain with a finite number N of the global modes selected in order to perform the dynamical model of the space vehicle.

5. Digital simulations

The simulations are performed with the following data:

$$\begin{aligned} A &= 9.5 \times 10^6 \text{ kg.m}^2; & B &= 10^6 \text{ kg.m}^2; & C &= 4 \times 10^6 \text{ kg.m}^2; & I &= 10^3 \text{ N.m}^2; & E &= \\ &10^3 \text{ N.m}^{-2}; & h &= 0,01 \text{ m}; & e &= 3,2 \text{ m}; & l &= 28,8 \text{ m}; & b &= 1,8 \text{ m}; & \tilde{m} &= 6 \text{ kg}; & P &= 140 \text{ N}; \\ \sigma &= 1,4 \text{ kg.m}^{-2}; & \rho &= 204 \text{ N.m}^{-3}; & \nu &= 0,3 \end{aligned}$$

I is the moment of inertia

N : Newton; m : meter; kg : kilogram;

5.1. Global modes gain

The convergence of the global modes gain is given by the equation (30). One defines the numerical sequence f_N :

$$f_N = \sum_{n=1}^N \theta_n^2.$$

As the global modes gain is convergent, the number N selected achieves a good approximation of formula (30). $N = 35$ is suitable to perform the numerical simulations in the following. The Figure 5 represents the simulation of the numerical sequence f_N .

5.2. Computation of the global eigenfrequencies

In the absence of external forces and orbital motion, the space vehicle lace attitude motion $\theta(t)$ is interacting with array bending in plane.

From equations (14), one computes the global modes eigenfrequencies φ_n corresponding to arrays bending in plane and the lace attitude of the space vehicle. In accordance with the modal gain approximation (30), 35

eigenfrequencies are selected in each case of global modes (see table 1).

Table 1: Global eigenfrequencies bending in plane in the bandwidth [0 – 4 Hz]

$\varphi_n/2\pi(\text{Hz})$												
0.100	0.179	0.201	0.397	0.495	0.579	0.597	0.695	0.298	0.793	0.893	0.992	1.091
1.184	1.199	1.289	1.389	1.487	1.686	1.785	1.884	1.587	1.983	2.017	2.084	2.182
2.281	2.380	2.479	2.578	2.678	2.776	2.876	2.974	3.068				

5.3. Calculation of the space vehicle global frequencies

Table 2: Global frequencies in band width [0 – 2 Hz]

n_0 (rad/s)	10^{-8}	10^{-7}	10^{-6}	10^{-5}	10^{-4}	10^{-3}
$\Omega/2\pi$ (Hz)	5.436×10^{-9}	5.43×10^{-8}	5.436×10^{-7}	5.436×10^{-6}	5.456×10^{-5}	2.777×10^{-4}
	1.412×10^{-8}	1.412×10^{-7}	1.412×10^{-6}	1.412×10^{-5}	1.419×10^{-4}	4.667×10^{-4}
	2.311×10^{-8}	1.875×10^{-7}	1.875×10^{-6}	1.875×10^{-5}	1.879×10^{-4}	8.938×10^{-4}
	2.602×10^{-8}	2.311×10^{-7}	2.311×10^{-6}	2.311×10^{-5}	2.331×10^{-4}	
	3.051×10^{-8}	2.602×10^{-7}	2.602×10^{-6}	2.605×10^{-5}	2.808×10^{-4}	
	3.473×10^{-8}	3.051×10^{-7}	3.051×10^{-6}	3.052×10^{-5}	3.120×10^{-4}	
	3.950×10^{-8}	3.473×10^{-7}	3.473×10^{-6}	3.476×10^{-5}	3.553×10^{-4}	
	4.359×10^{-8}	3.950×10^{-7}	3.950×10^{-6}	3.962×10^{-5}	4.098×10^{-4}	
	5.071×10^{-8}	4.359×10^{-7}	4.359×10^{-6}	4.369×10^{-5}	4.465×10^{-4}	
	5.276×10^{-8}	5.071×10^{-7}	5.071×10^{-6}	5.101×10^{-5}	5.155×10^{-4}	
	5.996×10^{-8}	5.276×10^{-7}	5.276×10^{-6}	5.313×10^{-5}	5.454×10^{-4}	
	6.722×10^{-8}	5.996×10^{-7}	5.996×10^{-6}	6.040×10^{-5}	6.110×10^{-4}	
	7.428×10^{-8}	6.722×10^{-7}	6.722×10^{-6}	6.779×10^{-5}		
	8.136×10^{-8}	7.134×10^{-7}	7.134×10^{-6}	7.143×10^{-5}		
	8.592×10^{-8}	7.428×10^{-7}	7.428×10^{-6}	7.458×10^{-5}		
	9.445×10^{-8}	8.136×10^{-7}	8.136×10^{-6}	8.174×10^{-5}		
	9.910×10^{-8}	8.592×10^{-7}	8.592×10^{-6}	8.621×10^{-5}		
	1.080×10^{-8}	9.445×10^{-7}	9.445×10^{-6}	9.475×10^{-5}		
	1.142×10^{-7}	9.910×10^{-7}	9.910×10^{-6}	9.938×10^{-5}		
	1.331×10^{-7}	1.080×10^{-6}	1.080×10^{-6}	1.081×10^{-4}		
5.503×10^{-7}	1.142×10^{-6}	1.142×10^{-6}	1.145×10^{-4}			
1.114×10^{-5}	1.331×10^{-6}	1.331×10^{-5}	1.334×10^{-4}			

One considers that the space vehicle undergoes orbital motion interacting with the lace attitude motion and the arrays deformations. In this case, one uses the spectral expansion (26) of the truncated impedance function $Z(\Omega)$ ($N = 35$) in accordance with the modal gain approximation (30). The natural global frequencies Ω of the whole space vehicle in absence of external torques, are computed from equation (29). Different values of the orbital parameter n_0 are considered to simulate the global frequencies of the whole space vehicle (see table 2). In the case of small angular speed n_0 of orders 10^{-8} , 10^{-7} , 10^{-6} and 10^{-5} in the bandwidth considered, one obtains for each order a spectrum of 22 eigenfrequencies Ω computed. On the other hand, the spectrum of eigenfrequencies obtained in work [12] where the attitudes motion are coupled, is very reduced. Since then, one notes a great interaction between the lace attitude motion and the vibrations of the space vehicle. Consequently, the model of attitude control suitable of the space vehicle should take into account the spectrum of lace attitude eigenfrequencies to avoid the resonance phenomena.

5.4. Graphical simulation of the array membrane deformations

Using the eigenfrequencies bending in plane φ_n , one simulates the different deformations of the array membrane. This simulations are represented in the figure 6, 7 and 8.

6. Conclusion

A previous work [12] has investigated the space vehicle using the spectral decompositions method. The global modes of the investigated space vehicle considering its attitudes motions coupled, are performed [12]. A reduced spectrum of the eigenfrequencies is obtained in this case. This fact is characterized by a small interaction between the coupled attitudes motions and the elastic deformations. Therefore, it is necessary to simulate a decoupling of the space vehicle attitudes motions in order to get a great interaction with the elastic deformations. Here, the decoupling of the space vehicle attitudes motion brings out the interaction between the lace attitude motions and the elastic deformations of the space vehicle. Consequently, one gets in this present study a great spectrum of the eigenfrequencies contrary to work [12]. This wide spectrum of the eigenfrequencies obtained here is necessary to perform a suitable model attitude control of the space vehicle in the practice.

References

- [1] H. B. Hablani. "Modal Analysis of Gyroscopic Flexible Spacecraft, a Continuum Approach." J. Guid 5 (5), pp. 448 – 457, 1982.
- [2] P. C. Hughes. "Dynamics of Flexible Space Vehicles with Active Attitudes Control." Celest. Mech. 9, pp. 21-39, 1974.
- [3] L. Meirovitch. "A Stationary Principle for the Eigenvalue Problem for Rotating Structures." AIAAJ. 14 (10), pp. 1387 – 1394, 1976.
- [4] M. Pascal. "Modal Analysis of a Rotating Flexible Space by a Continuum Approach." Z. Flug – wiss. Weltraumforsch. 18, pp. 395 – 401, 1994.
- [5] M. Pascal, M. Sylla. "Dynamic Model of a Large Space Structure by a Continuous Approach."

Recherche Aérospatiale N° 2, pp. 67 – 77, 1993.

[6] A. Sandu, D. Negrut, E. J. Haug, F.A. Potra, C. Sandu. "A Rosenbrock-Nystrom State Space Implicit Approach for the Dynamic Analysis of Mechanical System." Theoretical Formulation, J. Multibody Dyn. 217(4), 263 – 271, 2003.

[7] M. Sylla. "Spectral Decomposition Analysis Using the Global Modes of a Rotating Elastic Space Vehicle." Far East Journal of applied Mathematics 37(1), pp. 69 – 89, 2009.

[8] M. Sylla and B. Asseke. "Dynamics of a Rotating Flexible and Symmetric Spacecraft Using Impedance Matrix in Terms of the Flexible Appendages Cantilever Modes." Multibody System Dynamics. 19, pp. 345 – 364, 2008.

[9] M. Sylla and R. A. P. Barou. "A Mathematical Model of a Helicopter Standing and Rotating Rotor Blade." Far East Journal of applied Mathematics. 31(1), pp. 1 – 25, 2008.

[10] M. Sylla, M. Dosso and R. A. P. Barou. "Dynamical Analysis of a Flexible Mechanism by a Continuum Approach Using the Rotating Base Cantilever Modes." Far East Journal of Applied Mathematics. 33(2), pp. 187 – 204, 2008.

[11] M. Sylla and L. Gomat. "Modal Analysis of a Rotation Flexible Manipulator Arm." Afrika Matematika. Serie 3(19), 7 – 28, 2008.

[12] M. Sylla and S. J. M. KOUASSI. "Method of Modal Synthesis in the Dynamics of a Deformable Spatial Structure." Far East Journal of Dynamical Systems Volume 30(3), 103-133, 2018.

[13] M. Pascal. "La Stabilité d'Attitude d'un Satellite Muni de Panneaux Solaires." Acta Astronaut. 5, pp. 817 – 844, 1978.

- **Appendix 1**

Model description

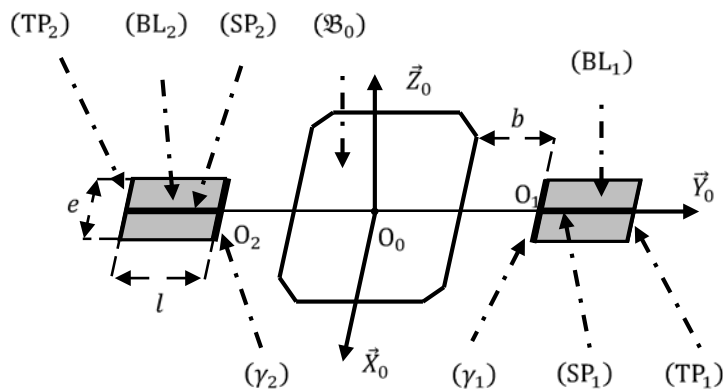


Figure 1: Satellite and solar arrays.

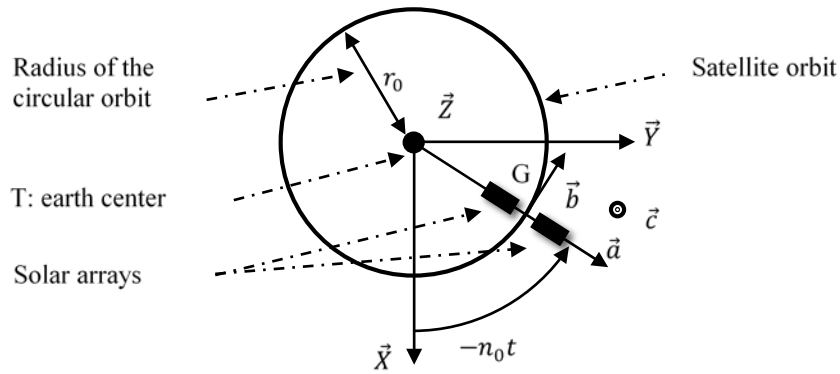


Figure 2: Satellite orbiting the earth.

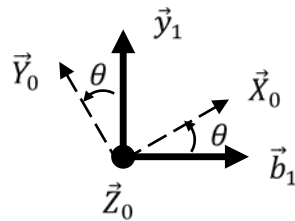


Figure 3: Attitude θ motion.

The angular velocity vector $\vec{\Lambda}$ of the reference frame \mathfrak{R} with respect to the reference frame \mathfrak{R}_T in $(G; \vec{X}_0, \vec{Y}_0, \vec{Z}_0)$ components is (figure 3):

$$\vec{\Lambda} = \begin{pmatrix} 0 \\ 0 \\ n_0 + \dot{\theta} \end{pmatrix}_{(\vec{x}_0, \vec{y}_0, \vec{z}_0)}$$

The elastic displacement fields modelling of the solar arrays investigated in works [4, 5, 8], is used here. Consequently, for each solar array (\mathfrak{B}_i) $i = 1, 2$ the elastic displacement field \vec{d}_i is:

$$\text{on } (SP_i), \quad \vec{d}_i(M, t) = (u_i(s, t), 0, 0)^T \quad s \in [0; l],$$

$$\text{on } (BL_i), \quad \vec{d}_i(M, t) = (\alpha_i(x, s, t), 0, 0)^T \quad (x, s) \in R.$$

Since the solar arrays are inextensible, the longitudinal displacement $v_i(s, t)$ and $\beta_i(x, s, t)$ is of second order and neglected in the linear theory [2, 3, 4]:

$$v_i(s, t) = -\frac{1}{2} \int_0^l \left[\left(\frac{\partial u_i}{\partial \zeta} \right)^2 \right] d\zeta ; \beta_i(x, s, t) = -\frac{1}{2} \int_0^l \left[\left(\frac{\partial \alpha_i}{\partial \zeta} \right)^2 \right] d\zeta.$$

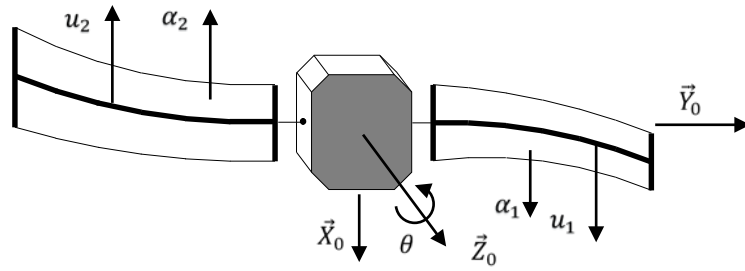


Figure 4: Bending in plane α_i, u_i of the solar arrays and lace attitude motion of the space vehicle.

• **Appendix 2**

The following variational principle of Hamilton is used to establish the motion equations [4, 5, 7, 8, 13].

$$\delta \int_{t_1}^{t_2} (K - V) dt = 0,$$

where K and V are, respectively, the kinetic and the total potential energy (including gravitational potential energy and the work of external torques) of the space vehicle.

$$V = \frac{n_0^2}{2} [3(A - B)\theta^2 + 6N_u^*\theta] + \tilde{\Pi}_D + \Upsilon\theta,$$

$$\tilde{\Pi}_D = \sum_{i=1}^2 \int_0^l \frac{EI}{2} \left(\frac{\partial u_i}{\partial s} \right)^2 - \frac{\tilde{P}}{2} \left(\frac{\partial u_i}{\partial s} \right)^2 ds + \sum_{i=1}^2 \iint_R \frac{\Gamma}{2} \left[\left(\frac{\partial \alpha_i}{\partial x} \right)^2 + \frac{1}{2} (\tilde{G} + \tilde{T}(s)) \left(\frac{\partial \alpha_i}{\partial s} \right)^2 \right] dx ds,$$

$$K = \frac{1}{2} [\vec{V}(G/\mathfrak{R}_T)]^2 + \vec{\omega} \cdot J_G(\vec{\omega}) + \int_{P \in (\mathfrak{B})} \overline{GP}^2 dm + 2\vec{\omega} \cdot \int_{P \in (\mathfrak{B})} \overline{GP} \wedge \dot{\overline{GP}} dm,$$

$$[\vec{V}(G/\mathfrak{R}_T)]^2 = (n_0 r_0)^2.$$

n_0 is constant orbital parameter.

Here J_G designates the inertia tensor in G

$$J_G = \begin{pmatrix} A + N_1 & N_4 & 0 \\ N_4 & B + N_2 & 0 \\ 0 & 0 & C + M_3 \end{pmatrix},$$

$$tr(J_G) = A + B + C + N_1 + N_2 + N_3,$$

$$N_1 = \sum_{i=1}^2 \left\{ - \int_0^l \frac{\tilde{P}_1(s)}{3n_0^2} \left(\frac{du_i}{ds} \right)^2 ds - \iint_R \frac{\tilde{T}_1(s)}{3n_0^2} \left(\frac{\partial \alpha_i}{\partial s} \right)^2 dx ds \right\},$$

$$N_2 = \sum_{i=1}^2 \left\{ \int_0^l \rho u_i^2 ds + \iint_R \sigma [\alpha_i^2 + 2x\alpha_i] ds dx + \tilde{m} u_i^2(l) \right\} - m_\Sigma X_G^2,$$

$$N_3 = \sum_{i=1}^2 \left\{ \int_0^l \rho u_i^2 ds + \iint_R \sigma [\alpha_i^2 + 2x\alpha_i] ds dx - \int_0^l \frac{\tilde{P}_1(s)}{3n_0^2} \left(\frac{du_i}{ds} \right)^2 ds - \iint_R \frac{\tilde{T}_1(s)}{3n_0^2} \left(\frac{\partial \alpha_i}{\partial s} \right)^2 dx ds + \tilde{m} u_i^2(l) \right\} - m_\Sigma X_G^2,$$

$$N_4 = \sum_{i=1}^2 (-1)^i \left\{ \iint_R x \frac{P_1(s)}{3n_0^2} \left(\frac{\partial \alpha_i}{\partial s} \right)^2 dx ds + \int_0^l \rho (b+s) u_i ds + \iint_R \sigma (b+s) \alpha_i ds dx + \tilde{m} (b+s) u_i(l) \right\}. \text{ Here:}$$

$$\tilde{P}_1(s) = 3\rho \frac{n_0^2}{2} [(b+l)^2 - (b+s)^2], \quad P_1(s) = \frac{n_0^2}{2} \left[\sigma(l-s) + \frac{\tilde{m}}{e} \right],$$

$$\tilde{T}_1(s) = 3 \frac{n_0^2}{2} \left[\sigma(b+l)^2 - \sigma(b+s)^2 + 2 \frac{\tilde{m}}{e} (b+l) \right],$$

$$\begin{cases} X_G = \frac{1}{m_\Sigma} \sum_{i=1}^2 \left[\int_0^l \rho u_i ds + \sigma \iint_R \alpha_i dx ds + \tilde{m} u_i(l, t) \right] \\ Y_G = \frac{1}{m_\Sigma} \sum_{i=1}^2 \left[\int_0^l \rho v_i ds + \sigma \iint_R \beta_i dx ds + \tilde{m} v_i(l, t) \right] \\ Z_G = 0 \end{cases},$$

m_Σ is the mass of the space vehicle.

Hence, the application of Hamilton's variational principle above, gives the linearized equations (1) to (10).

• **Appendix 3**

One introduces the expression of the deformations $u_i(s, t)$ (17) in the equation (3) of local motion (BL_i).

Taking into account the conditions (11), the expressions (13) and (6) one gets:

$$\rho \sum_{n=1}^{\infty} (-1)^i \theta_n [U_n^*(s) + (b+s)] [\dot{g}_n(t) + \varphi_n^2 g_n(t)] + 3n_0^2 \rho (-1)^i \sum_{n=1}^{\infty} \left[(b+s) - \frac{1}{2} [(b+l)^2 - (b+s)^2] U_n^{*'}(s) \right] \theta_n g_n(t) = -\rho (-1)^i (b+s) [\ddot{\lambda}(t) + 3n_0^2 \lambda(t)].$$

(a)

One multiplies the previous equation by $(-1)^i \theta_k U_k^*(s)$ then one integrates along (SP_i). After calculation one gets:

$$\sum_{n=1}^{\infty} \theta_n \theta_k \left\{ \left[\int_0^l \rho U_n^*(s) U_k^*(s) ds + \int_0^l \rho(b+s) U_k^*(s) ds \right] [\ddot{g}_n(t) + \varphi_n^2 g_n(t)] + 3n_0^2 \int_0^l \rho(b+s) U_k^*(s) ds g_n(t) \right\} + \frac{3}{2} n_0^2 \sum_{n=1}^{\infty} \theta_n \theta_k \int_0^l \tilde{P}_1^*(s) U_n^{*'}(s) U_k^{*'}(s) ds g_n(t) = -\theta_k \int_0^l \rho(b+s) U_k^*(s) ds [\ddot{\lambda}(t) + 3n_0^2 \lambda(t)].$$

One gets after some similar calculations the equations describing the motion of (BL_i) and the motion of (TP_i) . One makes the summation of these three equations. Using the equations of eigenfrequencies (13) and making a summation on i , the equation above becomes:

$$\sum_{n=1}^{\infty} \theta_n \theta_k \left[2 \left(\int_0^l \rho U_n^*(s) U_k^*(s) ds + \int_0^l \sigma e \alpha_n^*(s) \alpha_k^*(s) ds + \tilde{m} U_n^*(l) U_k^*(l) \right) - C \right] [\ddot{g}_n(t) + \varphi_n^2 g_n(t)] + 3n_0^2 \sum_{n=1}^{\infty} \theta_n \theta_k \left[\int_0^l \tilde{P}_1^*(s) U_n^{*'}(s) U_k^{*'}(s) ds + \int_0^l e \tilde{T}_1^*(s) \alpha_n^{*'}(s) \alpha_k^{*'}(s) ds - C \right] g_n(t) = C \theta_k [\ddot{\lambda}(t) + 3n_0^2 \lambda(t)].$$

One uses normalized orthogonality property (15) and the expression of m_{nk} (19):

$$\sum_{n=1}^{\infty} \delta_{nk} [\ddot{g}_n(t) + \varphi_n^2 g_n(t)] + 3n_0^2 \sum_{n=1}^{\infty} m_{nk} g_n(t) = C \theta_k [\ddot{\lambda}(t) + 3n_0^2 \lambda(t)].$$

• **Appendix 4**

One multiplies the previous equation by $(-1)^i(b+s)$ the equation (a) of the appendix 3, then one integrates along (SP_i) . After calculation one gets:

$$\sum_{n=1}^{\infty} \theta_n \left[\rho \int_0^l (b+s) U_n^*(s) ds + \rho \int_0^l (b+s)^2 ds \right] [\ddot{g}_n(t) + \varphi_n^2 g_n(t)] + 3n_0^2 \rho \sum_{n=1}^{\infty} \theta_n g_n(t) \left[\int_0^l (b+s)^2 ds + \frac{1}{2} \int_0^l [(b+l)^2 - (b+s)^2] U_n^{*'}(s) ds \right] = -\rho \int_0^l (b+s)^2 ds [\ddot{\lambda}(t) + 3n_0^2 \lambda(t)].$$

One gets after some similar calculations the equations describing the motion of (BL_i) and the motion of (TP_i) . One makes the summation of these three equations. Using the equations of eigenfrequencies (13) and making a summation, the equation above becomes:

$$[2\mathcal{L} - C] \sum_{n=1}^{\infty} \theta_n [\ddot{g}_n(t) + \varphi_n^2 g_n(t)] + 3n_0^2 \sum_{n=1}^{\infty} \theta_n C_n^* g_n(t) = -2\mathcal{L} [\ddot{\lambda}(t) + 3n_0^2 \lambda(t)].$$

with:

$$C_n^* = \int_0^l \tilde{P}_1^*(s) U_n^{*'}(s) ds + \int_0^l e \tilde{T}_1^*(s) \alpha_n^{*'}(s) ds + b e \tilde{T}_1^*(0) \alpha_n^{*'}(0) + 2\mathcal{L}.$$

One uses the equation of generalized coordinates (18) and after some manipulations:

$$\begin{aligned} \ddot{\lambda}(t) & \left[C(2\mathcal{L} - C) \sum_{n=1}^{\infty} \theta_n^2 + 2\mathcal{L} \right] \\ & + 3n_0^2 \left\{ \lambda(t) \left[C(2\mathcal{L} - C) \sum_{n=1}^{\infty} \theta_n^2 + 2\mathcal{L} \right] + \sum_{n=1}^{\infty} \theta_n \left[C_n^* g_n(t) - C(2\mathcal{M} - C) \sum_{p=1}^{\infty} m_{np} g_p(t) \right] \right\} \\ & = 0. \end{aligned}$$

The left side of the preceding equation which is a polynomial in n_0 is equal to zero whatever n_0 . One deduces:

$$\ddot{\lambda}(t) \left[C(2\mathcal{L} - C) \sum_{n=1}^{\infty} \theta_n^2 + 2\mathcal{L} \right] = 0$$

This equation is available whatever the parameter time t . Finally:

$$\sum_{n=1}^{\infty} \theta_n^2 = \frac{2\mathcal{L}}{C(C - 2\mathcal{L})}.$$

- **Appendix 5**

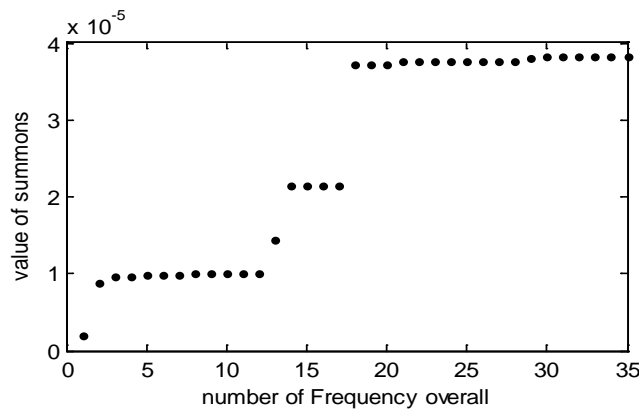


Figure 5: Representation of the function f_N as a function of N .

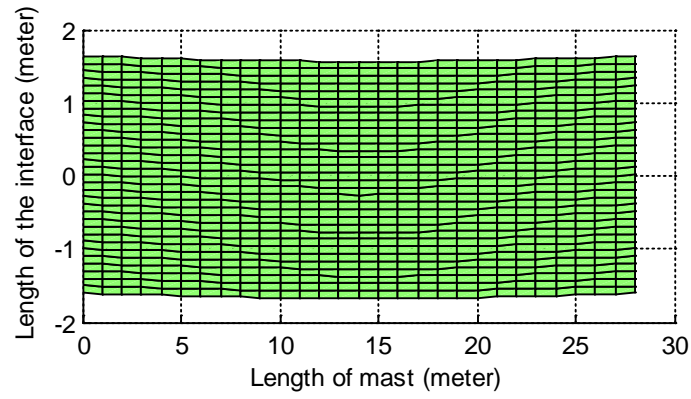


Figure 6: Deformation of the membrane solar arrays ($\varphi_n/2\pi = 0.1$ Hz).

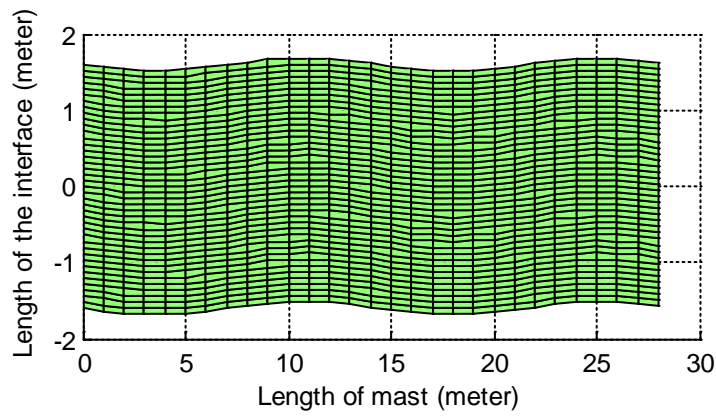


Figure 7: Deformation of the membrane solar arrays ($\varphi_n/2\pi = 0.597$ Hz).

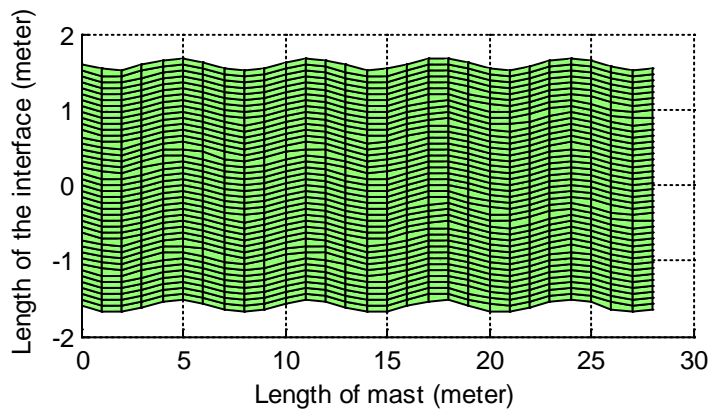


Figure 8: Deformation of the membrane solar arrays ($\varphi_n/2\pi = 1.090$ Hz).